

EFFECT OF HEATING ON THE STRUCTURE OF SYNTHETIC POROUS SILICA, MCM-41, SBA-15, and SBA-16

Shigeharu KITAKA, Satoshi KAWASAKI, and Shun KARIYA

*Department of Chemistry, Faculty of Science, Okayama University of Science,
1-1 Ridaicho, Kita-ku, Okayama 700-0005, Japan* e-mail: kittaka@mx3.tiki.ne.jp

(Received August 26, 2016; accepted December 5, 2016)

The effect of heating on the structural properties of synthetic porous silicas, MCM-41, SBA-15, and SBA-16, was studied by nitrogen and water adsorptions, and differential scanning calorimetry measurements of freezing and melting of pore water. The pore surface of MCM-41 was smoothed to decrease the surface area; however, the pore size was maintained almost unchanged on heating up to 900 °C. Micropores (coronas) of SBA-15 and SBA-16 are contracted at temperatures higher than 800 °C, and channel mesopores and the main pores are decreased in size

Key words: MCM-41; SBA-15; SBA-16; porosity; thermal treatment

Introduction

Silica is one of the most common materials in nature and for industrial uses. Its various properties are defined by the nature of the surface and the pore structure. Thermal treatment is a very strong method for changing the hydrophilicity of the pore surface and smoothing surface roughness. However, there have been no reports studying this subject. The present article reports the thermal stability and fragility of the pore structure of MCM-41, SBA-15, and SBA-16 using nitrogen and water adsorption, and by differential scanning calorimetry (DSC) measurements of the freezing and melting of pore water.

Experimental

Materials. MCM-41 was prepared by the method improved by Mori et al.^{1, 2)} Sample names may be found in the previous work.³⁾ SBA-15 and SBA-16 were prepared as in the previous work by Kittaka et al.⁴⁾ Numbers in the parenthesis signify the hydrothermal treatment temperature (°C) during sample preparation.

Heat treatment. Each sample was heated for 1 h using an electric furnace under vacuum.

Measurements. (a) Adsorption. Nitrogen adsorp-

tion on the MCM-41 was performed using a volumetric method at the temperature of liquid nitrogen, in which Baratron capacitance manometer 690A (MKS Japan) was used to measure the vapor pressure with vacuum valves automatically operated with high-pressure nitrogen from a cylinder with the aid of a home-made PC program. Nitrogen and water vapor adsorptions on SBA-15 and SBA-16 were measured gravimetrically with a Rubotherm adsorption balance (BEL, Japan) at the temperature of liquid nitrogen and at 298.2 K using a thermostatic water bath.³⁾ The adsorption system was controlled by use of home-made software operated with the Windows 98 operating system.

(b) DSC. Powder samples of MCM-41, SBA-15, and SBA-16 were dispersed in water in a test tube that had been linked with a vacuum line. By evacuating the suspension in the tube, the air in the pores was removed and suspending water was introduced instead. After the sedimented sample was placed in an aluminum DSC pan, excess water was lightly absorbed by use of filter paper. The DSC apparatus used is a Q10 (TA Instruments, USA). Measurements were conducted at the rate of 5 Kmin⁻¹ for both cooling and heating directions.

Results and Discussion

MCM-41 (C18). Figure 1 shows the plots of specific surface area and pore size of MCM-41 (C18) as a function of pretreatment temperatures. Specific surface area was determined on the adsorption isotherms of nitrogen in the front part before capillary condensation by applying the Brunauer–Emmett–Teller (BET) equation. Pore size was estimated on the desorption branch of the nitrogen isotherm by applying the technique developed by Dollimore and Heal.⁵⁾ Plotted values of both parameters are unchanged below the heating temperature of 600 °C, as expected by the fact that the sample used had been prepared by calcination at 600 °C. It is interesting that the surface

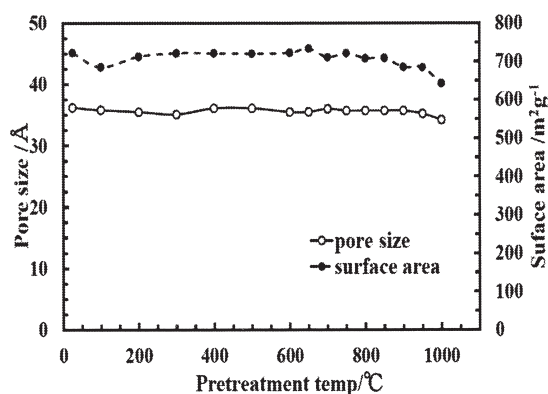


Fig. 1. Effect of heat treatment on the pore size and specific surface area of MCM-41(C18).

area decreased slightly but gradually above 600 °C, while the pore size was unchanged up to 900 °C. This gives us an image that the surface roughness of the cylindrical pores had been gradually smoothed and flattened. Thus one can understand that the main structure of MCM-41 is quite stable and is maintained up to 900 °C, above which the pore size decreased by thickening of the pore walls.

SBA-15: The form of the main pores of SBA-15 is imaged by hexagonally arranged cylindrical pores, which are connected with each other through thin channels. Furthermore, there are additional fine pores on the wall of the main pores and channels. These pores are micropores (coronas).⁴⁾ Figure 2a shows adsorption isotherms of nitrogen on SBA-15 (120, $d = 9.7$ nm) heated at 600, 800, 900, 950, and 1000 °C in a vacuum. Marked thermal effects appeared on the surface properties. The adsorption isotherm is a typical H1-type adsorption hysteresis of pore category, indicating that the material is cylindrically porous.⁶⁾

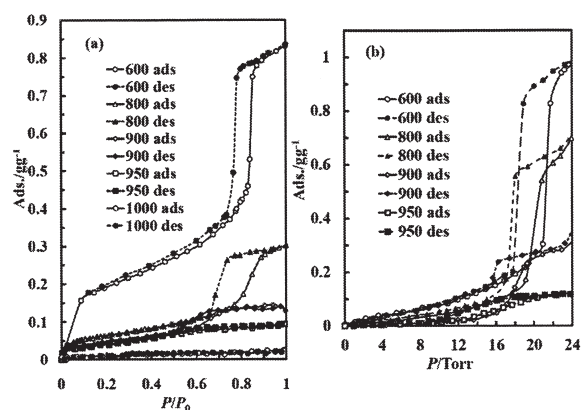


Fig. 2. (a) Adsorption isotherms of nitrogen at the temperature of liquid nitrogen on SBA-15 (120). (b) Adsorption isotherms of water on SBA-15 (120) at 298.2 K.

As the heating temperature is increased, the H1 form is deformed and capillary condensation pressure is displaced downward, and furthermore the amount of adsorption is decreased. These facts indicate a decrease in mesopore size, surface area, and deformation of pore shape with increase in temperature. It is anticipated that the micropores (coronas) disappeared simultaneously. Figure 2b for water adsorption shows a similar change of the adsorption isotherms on heating.

Figure 3 shows low-temperature DSC curves of water contacted with MCM-41 and heated SBA-15. Sharp exothermic peaks around 260 K are due to the freezing of external water. Small wavy external peaks at 240–230 K for MCM-41 (C14) are due to freezing of boundary water around porous particles between pore water and surrounding external water.⁷⁾ Large endothermic peaks are for the melting of external frozen water. The peaks before these are due to melting of frozen pore water. Freezing and melting temperatures of water confined in MCM-41 (C14) are lower than those for MCM-41 (C18), which can be explained by the Gibbs–Thomson effect involving the effect of pore size.³⁾ A similar relation can be seen for samples SBA-15 (80) and SBA-15 (100), which were prepared at 600 °C. A pore size decrease of SBA-15 on heating led to a similar freezing and melting temperature decrease here. Fragmentation of the freezing peak is ascribed to the less well-defined contraction of the pore structure. It is anticipated that various kinds of deformation processes are involved during heating at higher temperatures.

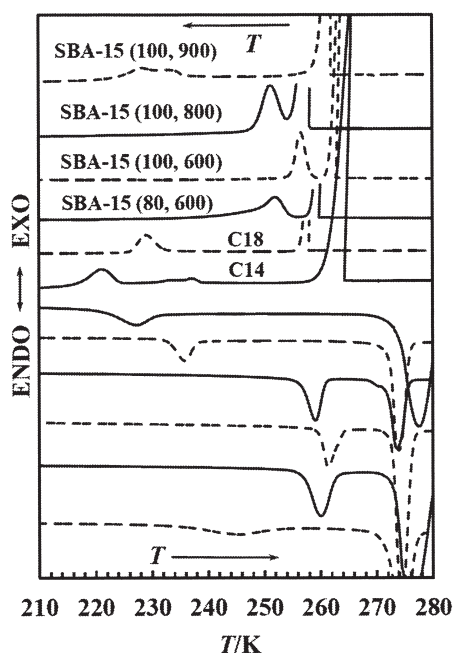


Fig. 3. Low temperature DSC curves of water contacted with MCM-41, SBA-15 (80) and heated SBA-15 (100). Scanning speed is 5 Kmin^{-1} . The numbers after the temperature of hydrothermal treatment during preparation are the calcination temperatures ($^{\circ}\text{C}$).

SBA-16: Adsorption isotherms. Figures 4a and 4b show the effects of heating on nitrogen and water adsorption, respectively, on SBA-16 (110). As-prepared SBA-16 (110, $d = 9.2 \text{ nm}$) shows vertical cavitation desorption at $P/P_0 = 0.5$, which is typical

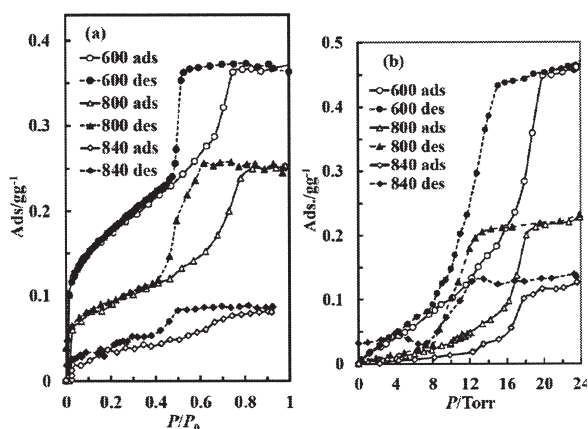


Fig. 4. (a) Adsorption isotherms of nitrogen on SBA-16 (110). (b) Adsorption isotherms of water on SBA-16 (110) at 298.2 K .

of the adsorption for the ink-bottle-type porous material.⁵⁾ As the heating temperature is increased, the hysteresis loop is gradually deformed together

with a decrease in adsorbed amount. The fact that the desorption starts at a higher pressure indicates that some portion of the outlet of the pore structure is partially enlarged.

The adsorption isotherm of water on SBA-16 (110) presents a rather complicated hysteresis loop. The starting material is composed of fairly large interconnecting channels and outlets for water adsorption. An increase in heat-treatment temperature decreased the outlet size. However, it is suggested that the similar pressures for adsorption and desorption steps are due to the remaining cages in the solid material. It is notable that by heating the sample at $840 \text{ }^{\circ}\text{C}$, the desorption of water is inhibited, even at low pressures, and thus thorough prolonged evacuation is needed for complete desorption.

DSC curves for freezing and melting behavior of water contacted with SBA-16 (110) and SBA-16 (120, $d = 11.0 \text{ nm}$) are shown in Figs. 5a and 5b, respectively. Large exothermic and endothermic peaks are

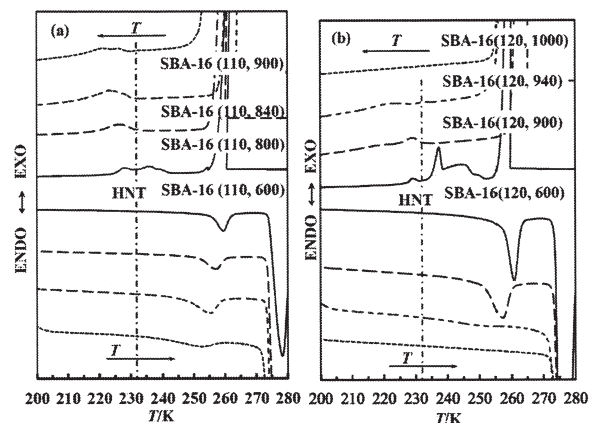


Fig. 5. (a) Low temperature DSC curves of water contacted with SBA-16 (110) heated at increasing temperatures. (b) SBA-16 (120). Scanning speed is 5 Kmin^{-1} . The numbers after the temperature of hydrothermal treatment during preparation are the calcination temperatures ($^{\circ}\text{C}$).

due to the external water as noted for Fig. 3. The water on the as-prepared samples shows complicated shapes for the freezing process. After freezing of external water, nucleation freezing of pore water propagates into spherical pores through the outlet of pores at temperatures above the homogeneous-nucleation temperature of water (HNT = 232 K). Water contacted with heated sample freezes at the HNT. This indicates that the outlet of the channel pores has been narrowed and water in it remains liquid even at the

HNT. When heated further at higher temperatures, a freezing peak appears at a temperature below the HNT. This indicates that the pore structure of the samples becomes less well defined with irregular pore shapes and narrower pore sizes, leading to deformed cylinders. The melting behavior is apparently simple with a single endothermic peak. This suggests that the melting process is gradual and not sensitive to the pore structure.

Thermal contraction of MCM-41 and SBA-15 and SBA-16. Figure 6 shows images of pore structure changes on heat treatment. In the case of MCM-41,

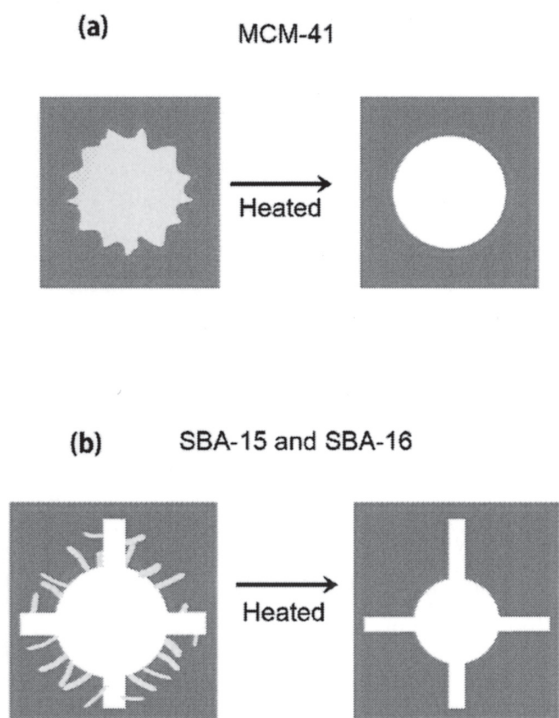


Fig. 6. Images of pore contraction of porous silica by heat treatment. (a) MCM-41(C18), (b) SBA-15 and SBA-16.

heat treatment above 600 °C leads to a slight decrease in specific surface area but small changes in pore size. This signifies that the surface roughness of as-prepared MCM-41 has been smoothed without significantly changing pore size, as shown in Figure 6a.

In the cases of SBA-15 and SBA-16, the dramatic changes in the structure of the adsorption isotherms and the decrease in adsorbed amount indicate two characteristic changes of pore structures. The micropores present on the pore surface (coronas) are eliminated, which leads to shrinkage of the silica

phases, which should lead to a decrease in the pore size, as shown in Figure 6b. It should also be noted that together with elimination of micropores, part of the interconnecting channels is thinned.

References

- 1) C. T. Kresge, M. E. Leonowicz, W. J. Roth, J. C. Vartuli, J. S. Beck, *Ordered mesoporous molecular sieves synthesized by a liquid-crystal template mechanism*, *Nature*, **359**, 710-712 (1992).
- 2) T. Mori, Y. Kuroda, Y. Yoshikawa, M. Nagao, and S. Kittaka, *Preparation of Water-resistant Siliceous MCM-41 Sample through Improvement of Surface Crystallinity, and Its Prominent Adsorption Features*, *Langmuir*, **18**, 1595-1603 (2002).
- 3) S. Kittaka, S. Ishimaru, M. Kuranishi, and T. Matsuda, T. Yamaguchi, *Enthalpy and interfacial free energy changes of water capillary condensed in mesoporous silica, MCM-41 and SBA-15*. *Phys. Chem. Chem. Phys.*, **8**, 3223-3231 (2006).
- 4) S. Kittaka, Y. Ueda, F. Fujisaki, T. Iiyama, and T. Yamaguchi, *Mechanism of Freezing of Water in Contact with Mesoporous Silicas MCM-41, SBA-15 and SBA-16: Role of Boundary Water of Pore Outlets in Freezing*. *Phys. Chem. Chem. Phys.*, **13**, 17222–17233 (2011).
- 5) D. Dollimore, and G. G. R. Heal, *An improved method for the calculation of pore size distribution from adsorption data*, *J. Appl. Chem.*, **14**, 199-114 (1964).
- 6) K. S. W. Sing and R. T. Williams, *Physisorption Hysteresis Loops and the Characterization of Nanoporous Materials*, *Ads. Sci. Tec.*, **22**, 773-782 (2004).
- 7) Shigeharu Kittaka, Kalyan Sou, Yamaguchi Toshio, and Ken-ichi Tozaki, *Thermodynamic and FTIR Studies on the Phase Changes of Water above and in Mesoporous MCM-41 before freezing of the Pore Water*, *Phys. Chem. Chem. Phys.*, **11**, 8538 – 8543 (2009).